口腔内における支台歯荷重の三次元解析に基づく部分床義歯設計の検討

口腔内における支台歯荷重の三次元解析に基づく部分床義歯設計の検討

課題番号　15390583

平成15年度～平成17年度科学研究費補助金（基盤研究(B)　）
研究成果報告書

平成18年5月

研究代表者　佐々木啓一
（東北大学　大学院歯学研究科　教授）

目次

1. はしがき

2. 研究組織

3. 交付決定額

4. 研究発表

5. 研究成果

6. 謝辞

7. 研究成果資料

1) In vivo 3-D force measurement on the abutment tooth of removable partial denture

2) 歯に加わる荷重の生体内三次元測定

3) In vivo 3-Dimensional force measurement in teeth during functions

4) Three-dimensional load on a tooth during function

5) In vivo 3-Dimensional measurement of the force exerted on a tooth during clenching

6) Behavior of 3-dimensional loads exerted on a tooth during function

7) Behaviors of 3-dimensional compressive and tensile forces exerted on a tooth during function

1. はしがき

部分床義歯の予後を決定する要素の一つとして，支台歯に加わる荷重があげられる．支台歯への負担過重は支台歯周組織に障害を及ぼし，義歯の予後を悪化させると考えられる．したがって，咀嚼や嚥下など機能時に義歯に加わる力の支台歯への伝播，および負担すべき荷重について知ることは，支台歯の選択を含めた義歯の設計や付与する咬合様式などを検討する上で極めて重要である．

今日までこの課題について数多くの研究が行われているが，その多くは光弾性模型や有限要素法による解析であり，患者個々の口腔内条件，すなわち支台歯や歯周組織の条件を詳細に反映する解析までは到達していない．また，口腔内において支台歯に加わる荷重を測定した研究はほとんどなく，三次元的に解析した研究は皆無であった．さらに，支台歯に加わる荷重に対しての支台装置の違いによる影響などについては未だ不明な点が多い．これらのことに結論を出すには，口腔内における荷重の実測が必要不可欠である．

最近，我々は精密加工と精密計測を専門とする工学分野との共同研究により，圧電性超小型荷重センサを歯の内部に組み込むことにより，機能時に歯へ作用する荷重を三次元的に実測し，機能力の口腔内分布をリアルタイムで解析可能な三次元荷重測定システムを開発した．

本研究では，このセンサを用いて種々の設計，形態の部分床義歯を装着した際の，機能時に支台歯へ作用する荷重とその変化を実測することにより，部分床義歯の設計，支台装置の種類ならびに咬合様式と支台歯に加わる荷重の関係を明らかにする．

さらに本システムを部分歯欠損患者に用いて、部分床義歯の設計や咬合の違いによる支台歯に作用する荷重の変化を検索し，支台歯に加わる機能力から見た義歯の設計について検討を加える。

本研究の結果は，これまでの部分床義歯における支台歯選択やクラスプの種類など支台装置の決定等に関する認識を変えうる可能性が高く，部分床義歯治療の予知性の向上に多大な貢献をもたらすものと考える．

2. 研究組織

研究代表者	佐々木啓一	(東北大学大学院歯学研究科・教授)
研究分担者	厨川常元	(東北大学大学院歯学研究科・教授)
	稲井哲司	(東北大学病院・講師)
	小山重人	(東北大学病院・講師)
	川田哲男	(東北大学大学院歯学研究科・助手)
研究協力者	川口威史	(東北大学大学院歯学研究科・大学院生)
	依田信裕	(東北大学大学院歯学研究科・大学院生)

3. 交付決定額

(金額単位 : 千円)

	直接経費	間接経費	合　計
平成15年度	4,600	0	4,600
平成16年度	4,800	0	4,800
平成17年度	2,300	0	2,300
総計	11,700	0	11,700

4. 研究発表

1) 川口威史, 川田哲男, 佐々木啓一, 厨川常元

小型水晶圧電式センサによる部分床義歯支台歯の荷重測定

第109回日本補綴歯科学会学術大会

品川区立総合区民会館「きゅりあん」(東京:平成15年5月11日)

2) Kawaguchi T, Kawata T, Sasaki K, Kuriyagawa T

In vivo 3-D force measurement on the abutment tooth of removable partial denture

The 10th meeting of the international college of prosthodontists

Hotel Nova scotia (Halifax: 2003 年 7 月 12 日)

3) 川田哲男, 依田信裕, 小川徹, 末永華子, 厨川常元, 佐々木啓一

歯に加わる荷重の生体内三次元測定

第38回日本エム・イー学会 東北支部大会

東北大学大学院工学研究科電子情報システム・応物系(仙台:平成16年 11月27日)

4) N Yoda, T Kawata, H Suenaga, T Kuriyagawa, K Sasaki

In vivo 3-Dimensional force measurement in teeth during functions

83rd General Session & Exhibition of the IADR

Baltimore Convention Center (Baltimore, 2005 年3月 10 日)

5) N Yoda, T Kawata, T Kawaguchi, H Suenaga, T Kuriyagawa, K Sasaki

Three-dimensional load on a tooth during function

International Symposium for Interface Oral Health Science in SENDAI

Sendai International Center (Sendai, 2005 年 2 月 2,3 日)

6) Kawata T, Yoda N, Suenaga H, Ogawa T, Kuriyagawa T and Sasaki K

Tractive force exerted on a tooth during chewing measured with 3-D transducer in vivo

The 11th meeting of the international college of prosthodontists

Creta Maris Resort (Crete: 2005 年 5 月 23 日)

7) N Yoda, T Kawata, T. Ogawa, T Kuriyagawa, K Sasaki

Behavior of 3-dimensional loads exerted on a tooth during function

The 4th Biennial Congress of Asian Academy of Prosthodontics

The Imperial Queen's Park Hotel (Bangkok: 2005 年 8 月 10 日)

5. 研究成果

1. Introduction

Functional occlusal forces transmitted onto teeth are determined by the biomechanical properties of the stomatognathic system, including the masticatory muscle forces, the position of the teeth, and the condition of the periodontal tissue. The transmitted force vectors are thus very complex. Numerous *in vitro* and *in vivo* studies have investigated the functional forces exerted in the mouth in order to identify the force magnitudes and directions related to the biomechanical conditions.

In vitro model simulations have been done using photoelastic models (Ralph and Caputo, 1975; Assif et al., 1989; Asundi and Anil, 2000) and two- or three-dimensional finite element models (Takahashi et al., 1980; Rees, 2001; Lee et al., 2002) and by means of strain gauges (Anderson, 1953; Craig and Peyton, 1966; Asundi and Anil, 2000). Photoelastic models have also been used to estimate the internal stress patterns. A major disadvantage of using such models is that the mechanical properties of plastic differ from those of periodontal tissue and jawbone. Finite element models can be used to estimate the ranges and distributions of stress and strain in a subject, although this requires using modules for the applied forces and knowing the property distributions of the muscles, jawbone, and periodontal tissue. In addition, the various power resources provided by the muscles of mastication are very difficult to reproduce.

Strain gauges have been used to register the direction and magnitude of strains under loading. However, because the tooth surface does not deform under normal physiological loads, attaching the points of a strain gauge to the surface of the tooth is not a suitable method for measuring imperceptible changes in the force magnitude and directions. As mentioned above, the transmitted force vectors are very complex. Since modeling results depend on the input data, *in vivo* data on the behavior of the forces should be used in the models. These forces have been measured with strain gauges in most *in vivo* studies. However, since the criteria for and definition of the tooth axis is vague and the shapes of the teeth crowns vary, it is difficult to conform the position of a strain gauge on a tooth surface to the other teeth. Therefore, few *in vivo* measurements have actually been carried out.

Since the spontaneous polarization that occurs in piezoelectric material corresponds to the load, a piezoelectric force transducer can accurately measure loads ranging from minute to intense. Such transducers have thus been used with many applications in the biomechanics field, which

requires accurate measurements (Collins and De Luca, 1994; Mitchell et al., 1995; Shiba et al., 1995; Goldie et al., 1996). Although application into the mouth has been attempted (Graf et al., 1974; Palla et al., 1981), measurement where the transducer is directly inserted into an abutment tooth crown has not yet been undertaken.

Functional forces transmitted to the abutment teeth of removable partial dentures are critical factors influencing the clinical results. Therefore, it is important to elucidate the functional forces onto the abutment tooth. There have been numerous studies discussing forces onto the abutment tooth. However, *in vivo* measurements have seldom been carried out, because of the difficulty of direct force sensing on a tooth during function.

The aim of this study was to insert a piezoelectric transducer into a tooth crown *in vivo* to measure the load applied to the tooth and to analyze the force magnitudes and directions with respect to the biomechanical conditions. We first clarified the characteristics of the piezoelectric force transducer to be used. Then we developed a measuring device for applying the transducer to a tooth. Finally, we measured the magnitudes and directions of a force applied to an abutment tooth of RPD and a tooth in natural dentition during function

2. Materials and Method

2.1. Measuring device

The functional load on the tooth was recorded using a 3-dimensional piezoelectric force transducer (Z18400, Kistler Instruments AG, Winterthur, Switzerland). It was an improved version of the piezoelectric force transducer used in studies of 3-dimensional force measurement on oral endosseous implants (Mericske-Stern et al. 1996a, 1996b, 1997, 1998) and was also water-resistant. It contained three crystals in a steel housing with a diameter of 7 mm and a height of 3.5 mm (Fig. 1a) for measuring the load along the x-, y-, and z-axes. The load could thus be simultaneously and independently measured in three dimensions, including the horizontal and perpendicular directions, in real time (Fig. 1b). The three dimensions were defined as vertical (z-axis), antero-posterior (y-axis), and mediolateral (x-axis). The transducer preloaded to 750 N had a horizontal measuring range of ±150 N (x-axis and y-axis) and a vertical one of ±500 N (z-axis). The measurement threshold was 0.01 N. Crosstalk along the x-axis was 0.1% in the direction of the z-axis and –0.6% in the direction of the y-axis. Along the y-axis, it was 1.1% in the direction of the x-axis and 1.7% in the direction of the z-axis. Along the z-axis, it was –0.1% in

the direction of the y-axis and –0.6% in the direction of the x-axis. These transducer specifications were provided by the manufacturer. The transducer charge was amplified using a 4-channel charge amplifier (5019B, Kistler Instruments AG, Winterthur, Switzerland), which was connected to the transducer with a multicore-shielded cable. The amplified signals were A/D converted using an A/D converter (NR-2000, Keyence Corporation, Osaka, Japan) with a sampling rate of 100 Hz and recorded on a personal computer.

2.2. Proofreading apparatus

The frame of the proofreading apparatus (Fig. 2a) used for benchmarking was manufactured from steel plate (15 mm thick) and had four steel pillars (15 mm square) so as not to be distorted by the applied load. A vise was attached to the frame. The angle of the vise could be shifted around one axis in 0.05° steps. Loading was done by placing weights, one by one, on a ball spline. The bottom end of the spline had a special probe so that the load transfer area was a point contact (Fig. 2b). A steel cap was secured to the brass jig at the end of the transducer using a steel screw to ensure that the pressure was distributed evenly over the pressure receiver of the transducer, which was the upper surface of the transducer (Fig. 1a). During horizontal measurement, the tip was set as close as possible to the pressure receiver (Fig. 2c).

2.3. Proofreading

The proofreading apparatus was used to clarify the characteristics of the piezoelectric force transducer under the assumption of oral conditions. The characteristics included 1) the relationship between the actual load and transducer output, 2) the effect of hysteresis on transducer output, and 3) the effect of temperature on transducer output.

The transducer was tightened with a 20-Ncm load to obtain a preload of about 680 N using an electric torque controller (DEA 055-0, Nobel Biocare, Göteborg, Sweden). The preload defined the measurement limitations in the perpendicular direction, permitting us to measure the tensile force. Moreover, it prevented the fixed transducer from sliding when horizontal shearing force was applied. The load when the tip of the ball spline contacted the cap on the transducer was defined as zero. Loads of up to 148, 148, and 297 N were applied to the x-, y-, and z-axes, respectively. To

measure the relationship between the actual load and transducer output, we applied the loads sequentially to each axis individually from zero to maximum in each trial. The number of different sequential loads applied to the x-, y-, and x-axes was 5, 5, and 8, respectively, in each of 10 trials. To measure the effect of hysteresis on transducer output, we applied the loads sequentially to each axis individually from zero to maximum and then sequentially removed them to reach zero again. The number of different sequential loads again applied to the x-, y-, and x-axes was 5, 5, and 8, respectively, in each of 10 trials, and the numbers were the same when removing them. The room temperature was 26° when the relationship between the actual load and transducer output and the effects of hysteresis on output were measured. The room temperature was changed from 26 to 38° in 2-degree increments when the effect of temperature on transducer output was measured. The loads were sequentially applied at each temperature in the same way as when the relationship between the actual load and transducer output was measured. The temperature of the transducer was maintained at each temperature for 10 minutes before measurement, and ten trials were carried out for each measurement condition. A thermocouple micro-probe (IT-21, Physitemp Instruments, Inc., NJ, USA) was attached to the transducer to measure the temperature. The temperature data were displayed on a microprobe thermometer (BAT-21, Physitemp Instruments, Inc., NJ, USA) and recorded on a personal computer.

2.4. Analysis

The data were analyzed using software for biological signal measurement and processing (Signal Basic Light 2100, Medical Try System Co.). Linear regression analysis was used to determine the relationship between the load and transducer output (STATISTICA, Stat Soft Inc, OK, USA).

2.5. Application into mouth

2.5.1. Device for 3-D force measurement

The piezoelectric force transducer was manufactured to fit into a commercial dental implant fixture (043.131S ITI standard implant, Straumann, Waldenburg, Switzerland). A custom-made

component was used to affix the transducer to a natural tooth. The measuring device comprised an inner part forming a metal core, the force transducer, and an outer part forming a metal tooth crown. The inner and outer parts were made of platinum gold cast alloy (Fig. 3a). These three parts were joined together with a steel screw (Fig. 3b). The implant fixture was embedded in the core to enable the transducer to be tightly fixed.

2.5.2 *In vivo* measurement

2.5.2.1 Natural dentition

The subject was a 26-year old healthy man having no abnormalities in the stomatognathic system. Informed consent was obtained after full explanation of this study. The load-measuring device was set over the maxillary left second molar, which had three roots and a root canal filling and was suitable for affixing the transducer. The palatal root was 7.8 mm long. The measuring device was inserted into the tooth root and held by temporary dental cement (Figs. 4a and b). Figure 4c shows the occlusal contact at the time of intercuspation.

The thermocouple micro-probe was attached to the metal tooth crown surface to measure the temperature. The temperature data were displayed on the microprobe thermometer and recorded on a personal computer.

The force magnitudes and directions in three dimensions were recorded during (MVC). The task was repeated five times. The 3-D load calculated from the outputs of the transducer was expressed as a vector of the coordinates based on the Frankfort horizontal plane (F-H plane) and sagittal plane. The starting point of the vector was the center of the pressure receiver. The transducer outputs were transformed using the angles calculated from posteroanterior and lateral cephalograms and a study cast. The palatal root was positioned at 29.0° to the perpendicular line of the F-H plane and 4.0° to the sagittal plane.

2.5.2.2 Partial edentulous dentition: abutment tooth

The subject was a sixty years old female with partial edentulous mandible. The right second premolar was needed for restoration after root canal treatment and it was adequate for setting the

transducer (Fig. 5). Her opposing dentition was a complete denture.

Figure 6 shows the artificial metal crown with the transducer. An experimental partial denture was provided the removable medial and distal rests (Fig. 7). The transmitted loads onto the abutment tooth were measured and compared among three different patterns of rest design, *i.e.* with medial rest, with the distal rest and both of the medial and distal rests. Experimental task employed in this study was maximum volúntary clenching (MVC). The task was repeated five times.

2.6. Transducer output transformation

The transducer outputs were based on the particular axis of the transducer (Fig. 1b). They needed to be transformed based on the reference axes defined in this study to clarify the relationship to the stomatognathic morphology. The anteroposterior axis (A-P) and mediolateral axis (M-L) were determined by the FH plane in the subject (Figs. 8a and b). The superior-inferior axis (S-I) was determined by a line perpendicular to the FH plane. The transformation regime was to first calculate the angle of the particular axes of the transducer to the reference axes at the first setout. The transducer output was then rotated three-dimensionally based on the angles calculated below.

Rotation angles α and β were estimated from the posteroanterior and lateral cephalograms (Figs. 8a and b). Rotation angle γ was estimated from the study cast, on which the transducer had been affixed (Fig. 8c).

The unit vector of the particular axis of the transducer (Figs. 8a, b, c) is given by

$$\mathbf{u} = [x \; y \; z]. \tag{1}$$

When the transformed output is **u'**, it can be written in matrix form as

$$\mathbf{u'} = \mathbf{u} \begin{bmatrix} 1 & 0 & 0 \\ 0 & \cos\alpha & \sin\alpha \\ 0 & -\sin\alpha & \cos\alpha \end{bmatrix} \begin{bmatrix} \cos\beta & 0 & -\sin\beta \\ 0 & 1 & 0 \\ \sin\beta & 0 & \cos\beta \end{bmatrix} \begin{bmatrix} \cos\gamma & \sin\gamma & 0 \\ -\sin\gamma & \cos\gamma & 0 \\ 0 & 0 & 1 \end{bmatrix}. \tag{2}$$

Figures 9a and b show examples of the raw output data obtained during MVC and the transformed output data in the natural dentition. Rotation angles α, β, and γ were 10.1, 16.0, and

51.5°, respectively.

3. Results

3.1. Proofreading

3.1.1 Relationship between transducer output and load (Fig. 10)

We applied linear regression analysis to the relationship between the transducer output and load. The correlation coefficients for the x-, y-, and z-axes were 0.99999, 0.99999, and 0.99996, respectively.

3.1.2 Effect of hysteresis on transducer output

The effect of hysteresis on transducer output was used to evaluate the reliability of transducer output when measuring dynamic loads, such as during mastication. The effects were 0.9%, 1.1%, and 1.7%, respectively, for the x-, y-, z-axes at maximum for ten trials. The effect of hysteresis on transducer output was thus negligible.

3.1.3. Effect of temperature on transducer output

A change in the temperature had little effect on transducer output. As the temperature was increased, the emitted charge increased. Most of the difference in transducer output occurred between 26 and 38°. The output at 38° increased 0.5%, 0.46%, and 0.45%, respectively, along the x-, y-, and z-axes, compared with that at 26°. The effect of temperature on transducer output was thus negligible.

3.2. Application into mouth

3.2.1 Natural dentition

As shown in Fig. 11a, during MVC, the compressive force exerted on the tooth increased rapidly from the start of clenching and reached a plateau. The rate of increase was 0.144 ± 0.034 N/msec, and the maximum force was 173.29 ± 15.32 N. Each axis's curve has a different point of the rising edge. As shown in Fig. 11b, during Caramel chewing, the force rhythmically increased

and decreased. The rate of increase was 0.977 ± 0.168 N/msec, and the maximum force was 146.3 ± 14.7 N. As shown in Fig. 11c, during peanut chewing, the force rhythmically increased and decreased, the same as during Caramel chewing. The duration of the chewing cycle was slightly longer than during Caramel chewing. The rate of increase was 0.363 ± 0.145 N/msec, and the maximum force was 57.7 ± 35.7 N. The maximum magnitude recorded during Peanut chewing was significantly smaller than that during MVC and Caramel chewing ($p < 0.001$, Dunn). There were no significant differences between MVC and Caramel chewing.

As the magnitude of the compressive force was increased, the vector tended toward the medial and posterior directions (Fig. 12). Viewed from the coronal plane, the maximum force vector was directed from the crown to the root medially at an angle of 10.27 ± 1.00° to the perpendicular line of the F-H plane (Fig. 12a). Viewed from the sagittal plane, the maximum force vector was directed from the crown to the root posteriorly at an angle of 3.18 ± 0.85° to the perpendicular line of the F-H plane (Fig. 12c). These directions were approximate to the direction of the palatal root, but not coincident with it, particularly anteroposteriorly. Compared to the palatal root, the maximum compressive force was directed posteriorly and laterally.

As the magnitude of the compressive force was increased, the force vector direction changed both in the coronal and sagittal plane for each type of chewing. For example, during Caramel chewing, the vector tended toward the medial (-11.4 ± 1.1°) and posterior (-3.7 ± 1.0°) directions (Fig. 13). The force vector direction at maximum magnitude in each cycle during Peanut chewing was significantly more laterally and widely scattered than that during MVC and Caramel chewing ($p < 0.01$, Dunn) (Fig. 14). There were no significant differences between MVC and Caramel chewing. The range of the force vector direction during the force-increasing phase of MVC was significantly smaller than that during Caramel chewing and Peanut chewing, both in the coronal and sagittal planes ($p < 0.01$, Dunn) (Fig. 15).

The tensile force was recorded throughout the second half of Caramel chewing but not during MVC and peanut chewing (Figs. 13 and 16). It reached a maximum (on average) 0.161 ± 0.034 msec after the compressive force reached a maximum during each chewing cycle (Fig. 16). The maximum magnitude of the tensile force was 4.05 ± 0.98 N (range: 2.05–6.37 N). The direction was 45.7 ± 11.5° anteriorly and 11.6 ± 17.3° laterally. The tensile force was dispersed significantly wider than the compressive force ($P < 0.001$, Mann-Whitney) (Fig. 17).

3.2.2 Partial edentulous dentition

The direction and amplitude of the transmitted forces onto the abutment tooth in the sagittal plane and projected on the lateral cephalogram (Fig. 18a). The mean values of the direction and amplitude of the loads measured at four directions i.e. without denture, wearing the experimental denture with the medial and distal rests, with the medial rest and with the distal rest are shown in Table 1. The force vector without denture directed more posteriorly than the vectors at wearing the denture. Among three different conditions of rest design, the force vector with the distal rest was towards the most posterior direction. The angles decreased in descending order when measured with the medial and distal rest, and with the medial rest. There was significant difference between the angles with the medial rest and with the distal rest. As for the maximum load, highest force was recorded when not wearing the denture. Meanwhile, the smallest force was recorded when the denture with the distal rest was worn. Force vectors of the transmitted forces are projected on the P-A cephalogram (Fig. 18b). The mean values of direction and amplitude of the force vectors in the frontal plane at four different conditions are shown in Table 2. The force vector with the medial and distal rests directed most laterally, and that with the medial rest directed most downward. There was not significant difference among the directions of four different conditions in the frontal plane.

4. Discussion

Many measurements of a load applied to teeth have been done *in vivo* and *in vitro*. Because *in vivo* measurements are problematic due to the transducer size, *in vitro* measurements have been done more often. Since the phenomena can be interpreted very easily, *in vitro* measurements can simplify the experimental conditions. The results derived from *in vivo* measurements are complicated due to the many power resources provided by the muscles of mastication and the flexibility of the constituent elements, including the periodontal membrane and jaw bone (Korioth and Hannam, 1994; Koolstra and van Eijden, 2001). While *in vitro* measurements have thus been more common, thorough analysis of the results requires knowledge of the original transmission attitudes of the loads *in vivo*. Furthermore, the 3-D loads, both magnitude and direction, need to be measured. Since we were able to insert the transducer directly into a tooth, we could directly measure the 3-D load applied to it. We still need to measure the *in vivo* accuracy of this transducer.

As the correlation coefficients between the loads and transducer output were 0.99999 for the x-axis, 0.99999 for the y-axis, and 0.99996 for the z-axis, the relationship for each axis showed very good linearity. The slightly worse coefficient for the z-axis was because the z-axis had twice as much load applied as the other axes. These linearities for the transducer outputs demonstrate

that the data output by the transducer were valid. The correlation coefficients were higher than for results obtained with a similar transducer (Mericske-Stern et al., 1996a) that used half the preload we used. In the latter study, the authors needed to apply the preload when the transducer was in the mouth, consequently they had to use a lower preload. Our ability to preload the transducer when it was outside the mouth resulted in better correlation between the load and output

Hysteresis of the transducer output along each axis had very little effect. The principal factor responsible for hysteresis was apparently the use of a housing made of steel rather than one made of crystal, which is the main part of the transducer. The results demonstrated the reliability of the transducer output with a variable load. The finding that the output was little affected by hysteresis means that the transducer is well suited for measuring dynamic loads.

A piezoelectric element emits electric charges due to loading. An increase in the temperature increases the electric charge. The higher the temperature, the more easily electric charges are emitted. We initially thought that this transducer might be greatly affected by temperature. The outer crown where the transducer was installed experienced temperature changes when the subject's mouth was open. We thus measured the difference in transducer output between room temperature and mouth temperature. We found that changes in temperature had an insignificant effect on output under measurement conditions that were consistent with use in the mouth.

To the best of our knowledge, this study is the first to establish a method for *in vivo* 3-dimensional measurement of the force exerted on a tooth during function. While another group (Mericske-Stern et al. 1996a, 1996b, 1997, 1998) applied a similar transducer to implant-borne dental prostheses, we applied our transducer to a tooth having a vital periodontal ligament and viable periodontium. Moreover, we transformed the transducer output to clarify the force direction relative to a skeletally based coordinate system. The clinical situation differs greatly from that of an endosseous implant because the periodontal ligament is known to be an important component of neurosensory systems for detecting forces exerted on human teeth (Trulsson and Johansson, 1994, 1996). We used the FH plane as the coordinate basis in this study. The use of this basis should help elucidate the biomechanics of the stomatognathic system in relation to cranio-facial morphology and help clarify the functional meanings of force exerted on the tooth in relation to stomatognathic function. In the future, the force vectors for different teeth need to be compared, and the interindividual differences need to be clarified using the skeletal reference.

While this transducer cannot be used on all teeth, it can be inserted into any tooth that has had endodontic treatment, has a crown more than 5 mm high and more than 7 mm wide, and has a root canal more than 2 mm wide. When these conditions are met, this transducer can be used to

measure the load applied to the tooth *in vivo*. Having succeeded in applying this transducer to in-mouth measurement, we will next test its ability to dynamically measure a load applied to a tooth under function.

Applying this measuring system to the subjects, numerous findings as to the transmitted forces onto the subject teeth could be obtained, which were unable to be demonstrated before. The change in the compressive force vector during both chewing and clenching is explained as follows. During clenching at the intercuspal position, forces generated by the masticatory muscles are exerted on the upper and lower dentitions as well as on the bilateral temporomandibular joints (Korioth and Hannam, 1994a, 1994b). The force vector on a tooth is a component of the forces exerted on the total dentition. Thus, the changes in the force vector on the subject tooth would reflect the balance and changes in the force vectors on the total dentition based on the muscle function (Eriksson et al., 1984, Blanksma et al., 1992, Hannam and McMillan, 1994, Ogawa et al, 2006). Masticatory muscles' activities naturally change during clenching. However, since the rate of increase in both the masseter (Devlin and Wastell, 1985) and temporalis (Mao et al., 1996) activity is not coincident with that of the occlusal force magnitude, there must be another explanation. Because the timing of the medial pterygoid does not coincide with that of the masseter and temporalis for several jaw functions (Hannam and Wood, 1981, Wood, 1981, Plesh et al, 1996), the medial pterygoid may have contributed to the change in the compressive force vector. The change during clenching might be related to the movement of the tooth, which depends on the viscoelastic character of the periodontium and the distortion of the alveolar bone (Korioth and Hannam, 1994a, 1994b). The upper molar apparently displaces in the root direction and tilts toward the palatal direction during clenching (Kato, H., 1982, Miura et al., 1995). Kato reported that the measurement point on the tooth crown moved 61–116 micrometers in the palatal direction during clenching when the compressive force was 20–46 kgf, so the changes in the alignment angle of the tooth axis are not clear in their results. In contrast, the direction of the changes in the compressive force in the present study was largely coincident with the direction of the tooth movement. The change in the tooth alignment and the forces and movements caused by adjacent contacted tooth during clenching might therefore partly contribute to the force vector changes we recorded. The difference in the vector direction between the force-increasing phase and the force-decreasing phase of MVC may be related to the mechanical properties of the periodontal membrane and the alveolar, as the periodontal membrane has viscoelastic conforming compression and decompression and the alveolar bones distorted during function.

As the magnitude of the compressive force increased during both MVC and caramel chewing,

the vector direction of the force at maximum magnitude concentrated, and the mediolateral direction of the force tended to correspond to the direction of the palatal root of the tooth. This supports the general concept of the relationship between the tooth axis and an occlusal force (Kato, H., 1982, Miura et al., 1995). In contrast, the vector direction at maximum tensile force during caramel chewing was dispersed. This might be related to the position of the item to be chewed on the tooth before opening the mouth.

Compressive force was apparently applied to the tooth from various directions during chewing. As a result, the range of the force vector direction during caramel chewing and peanut chewing was significantly larger than that during MVC during the force-increasing phase.

Since the maximum compressive force during peanut chewing was smaller and more dispersed than during Caramel chewing in most chewing cycles, the mandibular position during peanut chewing might have been dispersed. Additionally, for hard foods like peanuts, the compressive force applied to a tooth during chewing might vary due to food remnants between the occlusal surfaces of the maxillary and mandibular teeth. These remnants might account for our finding that the range of the vector direction at maximum magnitude during peanut chewing was wider than that during Caramel chewing.

To the best of our knowledge, this study is the first to measure the tensile force exerted on a tooth during function, i.e., Caramel chewing; this force was not recorded during MVC and peanut chewing. It goes without saying that the characteristics of the food item, such as stickiness, affect the tensile force generated. As tensile force can lead to the loss of a restoration or prosthesis, this data should be helpful for research in those areas.

The actual tensile force was probably more than 4 N because large tensile force is usually felt when chewing sticky food. This speculation is supported by our finding that the rate of decrease in the compressive force during the opening phase of Caramel chewing (0.958 ± 0.147 N/msec) was significantly larger than during simply opening the mouth (0.443 ± 0.084 N/msec). This indicates that force was applied to the tooth during Caramel chewing; that is, the tensile force developed soon after maximum compressive force occurred. Given that the tensile force started at the onset of the maximum compressive force (① in Fig. 7a), the force was larger, possibly greater than 150 N (roughly 4+146 N), than the value recorded (4.05 ± 0.98 N) in this study.

We used the F-H plane as the coordinate basis, which should help elucidate the biomechanics of the stomatognathic system in relation to cranio-facial morphology and help clarify the functional meanings of force exerted on the tooth in relation to stomatognathic function. We still need to compare the force vectors for different teeth and clarify the interindividual differences

using the skeletal reference.

Our finding that the compressive force direction at the maximum magnitude was approximate to the direction of the palatal root but not coincident with it is probably related to the biomechanics of the stomatognathic system. In particular, the characteristics of the facial skeleton, the lines of action of the muscles, and the physiology of the muscles, including that within the muscles (Eriksson et al., 1984, Blanksma et al., 1992, Hannam and McMillan, 1994, Ogawa et al, 2006), probably affect the direction. Further investigation is needed to clarify the differences in direction.

The magnitude of transmitted force onto the abutment tooth was higher in measurement without the RPD than with the RPD with any types of rest design. The direction of force vector without the RPD was more posteriorly than with the RPD. Among three different rest designs, the vector with the distal rest was toward the most posterior direction, followed with the medial and distal rest, and with the medial rest, in order. Regarding the force direction in the frontal plane, significant differences were not observed among the conditions.

When applying RPD for restoration in the distal free-ending edentulous ridges like as the case in the subject, design of RPD, especially the rest setting onto the abutment tooth is considered as one of the critical points of discussion in order to protect the abutment tooth and supporting tissues. Numerous studies have been, therefore, made discussing RPD design and the force onto the abutment tooth and residual ridges, and movement of the abutment tooth and the denture base (Matsumoto, 1970, Thompson, 1977, McCartney, 1980, Firtell, 1985, Bazirgan, 1986, Ogata, 1992, Igarashi, 1999). Although the ideal theories of RPD designing for protecting the abutment teeth and residual tissues have been proposed (Boucher, 1982, McGivney, 1995), the direct measurement of the transmitted forces onto the abutment tooth in vivo has not been carried out yet. The findings in this study are the first descriptions as to the forces onto the abutment tooth in vivo. In the results, it is indicated that wearing RPD decreased the force, which would be related to shearing the occlusal force onto the residual ridge via the denture base as described in the textbooks. The differences of the force vector onto the abutment tooth relating to the rest designs are also coincident with the descriptions in the textbooks (Boucher, 1982, McGivney, 1995). However, this study could reveal the actual measurement values of magnitudes and directions of forces. It would be distinctly valuable for establishing RPD designing based on biomechanics and biology.

Our force-measuring device can be used to measure *in vivo* both the compressive and tensile 3-D force exerted on a tooth during function over time. Application of this device to a greater number of subjects will provide important basic data for clarification of stomatognathic functions

and for analysis using computer simulation, such as finite element analysis.

5. Conclusions

The 3-D force-measuring device we developed with a piezoelectric transducer has high responsibility and thermal stability in the mouth. Using the device, we recorded the 3-D compressive and tensile forces exerted on a tooth during function, although only for one subject. We found that the direction of the forces changed during function, both during chewing and maximal voluntary clenching. There were significant differences in the behavior of the forces. The characteristics of the item chewed affected the force vector. The force transmitted to the abutment tooth of RPD differed within rest resign.

The device enabled time series measurement of the dynamic load on a tooth during function *in vivo*. Its use should help clarify the biomechanical characteristics of the stomatognathic system and establish the design of the RPD.

References

Anderson, D.J., 1953. A method of recording masticatory loads. Journal of Dental Research 32, 785–789.

Assif, D., Oren, E., Marshak, B.L., Aviv, I., 1989. Photoelastic analysis of stress transfer by endodontically treated teeth to the supporting structure using different restorative techniques. Journal of Prosthetic Dentistry 61, 535–543.

Asundi, A., Anil, K., 2000. A strain gauge and photoelastic analysis of in vivo strain and in vitro stress distribution in human dental supporting structures. Archives of Oral Biology 45, 543–550.

Bazirgan, M., Bates, J., 1986. Preliminary study of a method of measuring removable partial denture abutment tooth movement in vitro and in vivo. Journal of Prosthetic Dentistry 56, 204–207.

Blanksma, N.G., van Eijden, T.M.G.J., Weijs, W.A., 1992. Electromyographic heterogeneity in the human masseter muscle. Journal of Dental Research 71; 47–52.

Boucher, L.J., Renner, R.P., 1982. Treatment of partially edentulous patients 1st edn, 5.C.V. Mosby Inc, New York.

Collins, J.J., De Lucaramel chewing.J., 1994. Random walking during quiet standing. Physical

Review Letters 73, 764–767.

Craig, R.G., Peyton, F.A., 1966. Measurement of strains in fixed bridges with electronic strain gauges. Journal of Dental Research 46, 615–619.

Devlin, H., Wastell, D.G., 1985. Bite force and masseter muscle electromyographic activity during onset of an isometric clench in man. Archives of Oral Biology 30; 213–215.

Eriksson, P-O, Stalberg, E., Antoni, L., 1984. Flexibility in motor-unit firing pattern in the human temporal and masseter muscles related to type of activation and location. Archives of Oral Biology 29; 707–712.

Firtell, D.N., Grisius, R.J., Muncheryan, A.M., 1985. Reaction of the anterior abutment of Kennedy class □ removable partial denture to various clasp arm designs: an in vitro study. Journal of Prosthetic Dentistry 53, 77–82.

Goldie, P.A., Matyas, T.A., Evans, O.M., Galea, M., Bach, T.M., 1996. Maximum voluntary weight-bearing by the affected and unaffected legs in standing following stroke. Clinical Biomechanics 11, 333–342.

Graf, H., Grassl, H., Aeberhard, H.J., 1974. A method for measurement of occlusal forces in three directions. Helv. Odont. Acta 18, 7–11.

Igarashi, Y., Ogata, A., Kuroiwa, A., Wang, C.H., 1999. Stress distribution and abutment tooth mobility of distal-extension removable partialdentures with different retainers: an in vitro study. Journal of Oral Rehabilitation 26, 111-116.

Hannam, A.G., McMillan, A.S., 1994. Internal organization in the human jaw muscles. Critical Reviews of Oral Biology and Medicine 5; 55–59.

Hannam, A.G., Wood, W.W., 1981. Medial pterygoid muscle activity during the closing and compressive phases of human mastication. American Journal of Physiology and Anthropology 55; 359–367.

Koolstra, J.H., van Eijden, T.M.G.J., 2001. A method to predict muscle control in the kinematically and mechanically indeterminate human masticatory system. Journal of Biomechanics 34, 1179–1188.

Korioth, T.W.P., Hannam A.G., 1994a. Deformation of the human mandible during simulated tooth clenching. Journal of Dental Research 73; 56–66.

Korioth, T.W.P., Hannam, A.G., 1994b. Mandibular force during simulated tooth clenching. Journal of Orofacial Pain 8, 178–189.

Lee, H.E., Lin, C.L., Wang, C.H., Cheng, C.H., Chang, C.H., 2002. Stresses at the cervical lesion of maxillary premolar—a finite element investigation. Journal of Dentistry 30, 283–290.

Mao, J.J., Major, P.W., Osborn, J.W., 1996. Coupling electrical and mechanical outputs of human jaw muscles undertaking multidirectional bite-force tasks. Archives of Oral Biology 1996; 41; 1141–1147.

Matsumoto, M., Goto, T., 1970. An experimental investigation in design and force distribution with unilateral mandibular distal extension removable partial dentures. Bulletin of the Tokyo Medical Dental University 17, 113–.

McCartney, J.W., 1980. Motion vector analysis of an abutment for a distal-extension removable partial denture: a pilot study. Journal of Prosthetic Dentistry 43, 15–21.

McGivney, G.P., Castleberry, D.J., 1995. McCracken's removable partial prosthodonthics, 9th edn. 166,331. C.V. Mosby Inc, New York.

Mericske-Stern, R., Assal, P., Buergin, W., 1996a. Simultaneous force measurements in 3 dimensions on oral endosseous implants in vitro and in vivo. Clinical Oral Implants Research 7, 378–386.

Mericske-Stern, R., Piotti, M., Sirtes, G., 1996b. 3-D in vivo force measurement on mandibular implants supporting overdentures. Clinical Oral Implants Research 7, 387–396.

Mericske-Stern, R., 1997. Force distribution on implants supporting overdentures: the effect of distal bar extensions. Clinical Oral Implants Research 8, 142–151.

Mericske-Stern, R., 1998. Three-dimensional force measurement with mandibular overdentures connected to implants by ball-shaped retentive anchors. A clinical study. International Journal of Oral & Maxillofacial Implants 13, 36–43.

Mitchell, S.L., Collins, J.J., De Lucaramel chewing.J., Burrows, A., Lipsitz, L.A., 1995. Open-loop and closed-loop postural control mechanisms in Parkinson's disease: increased mediolateral activity during quiet standing. Neuroscience Letters 197, 133–136.

Ogata, K., Ishii, A., Nagare, I., 1992. Longitudinal study on torque transmitted force from a denture base to abutment tooth of a distal extension removable partial denture with circumferential clasps. Journal of Oral Rehabilitation 19,245-252.

Ogawa, T., Kawata, T., Tsuboi, A., Hattori, Y., Watanabe, M., Sasaki, K., 2006. Functional properties and regional differences of human masseter motor units related to three-dimensional bite force. Journal of Oral Rehabilitation, in press.

Plesh, O., Bishop, B., McCall, W.D., 1996. Patterns of jaw muscle activity during voluntary chewing. 23; Journal of Oral Rehabilitation 262–269.

Ralph, J.P., Caputo, A.A., 1975. Analysis of stress patterns in the human mandible. Journal of Dental Research 54, 814–821.

Rees, J.S., 2001. An investigation into the importance of the periodontal ligament and alveolar bone as supporting structures in finite element studies. Journal of Oral Rehabilitation 28, 425–432.

Palla, S., Bailey, J.O., Grassl, H., Ash, M.M., 1981. The effect of bite force on the duration and latency of the menton tap silent period. Journal of Oral Rehabilitation 8, 243–253.

Shiba, N., Kitaoka, H.B., Cahalan, T.D., Chao, Y.S.E., 1995. Shock-absorbing effect of shoe insert materials commonly used in management of lower extremity disorders. Clinical Orthopaedics and Related Research 310, 130–136.

Takahashi, N., Kitagami, T., Komori, T., 1980. Behaviour of teeth under various loading conditions with finite element method. Journal of Oral Rehabilitation 7, 453–461.

Thompson, W.D., Kratchvil F.J., Caputo, A.A., 1977. Evaluation of photoelastic stress patterns produced by various designs of bilateral distal extension removable partial dentures. Journal of Prosthetic Dentistry 38; 261-273.

Trulsson and Johansson, 1994. Encoding of amplitude and rate of forces applied to the teeth by human periodontal mechanoreceptive afferents. Journal of Neurophysiology 74, 1734–1744.

Trulsson and Johansson, 1996. Encoding of tooth loads by human periodontal afferents and their role in jaw motor control. Progress in Neurobiology 49, 267–284.

Wood, W.W., 1986. Medial pterygoid muscle activity during chewing and clenching. Journal of Prosthetic Dentistry 55; 615–621.

Kato, H., 1982 The function of tooth supporting structures. Part II. The dynamics of molars in function and at rest. The Journal of Japan Prosthodontic Society (in Japanese) 26; 133–147.

Miura, H., Hasegawa, S., Kato, H., Furuki, Y., Masuda, T., 1995. A measuring method of the three dimensional tooth displacement. The Journal of Japanese Society of Stomatognathic Function (in Japanese) 2; 1–10.

Figure

Fig. 1

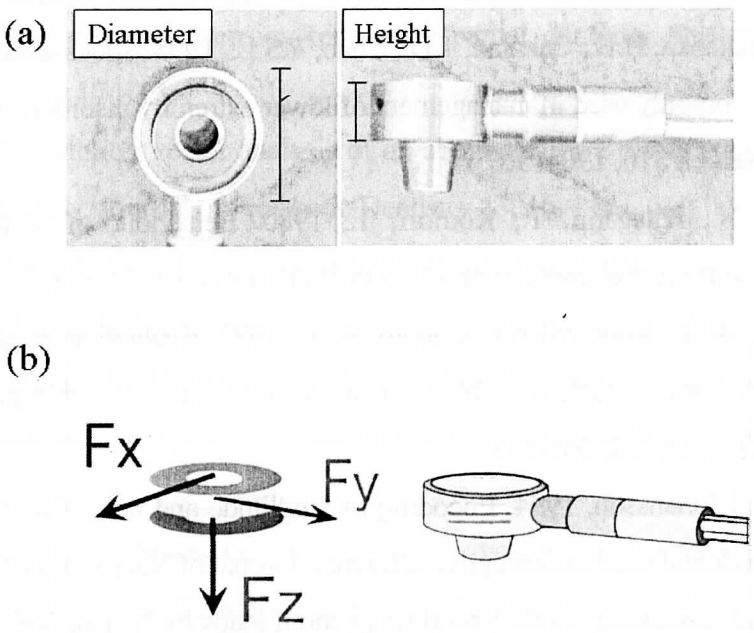

Fig. 1 Structure of piezoelectric 3-component force transducer:
(a) diameter is 7 mm, and height is 3.5 mm; (b) three crystals in steel housing enable loads to be simultaneously and independently measured in three directions (along x-, y-, and z-axes). Upper surface of transducer is pressure receiver (diameter 5 mm).

Fig. 2

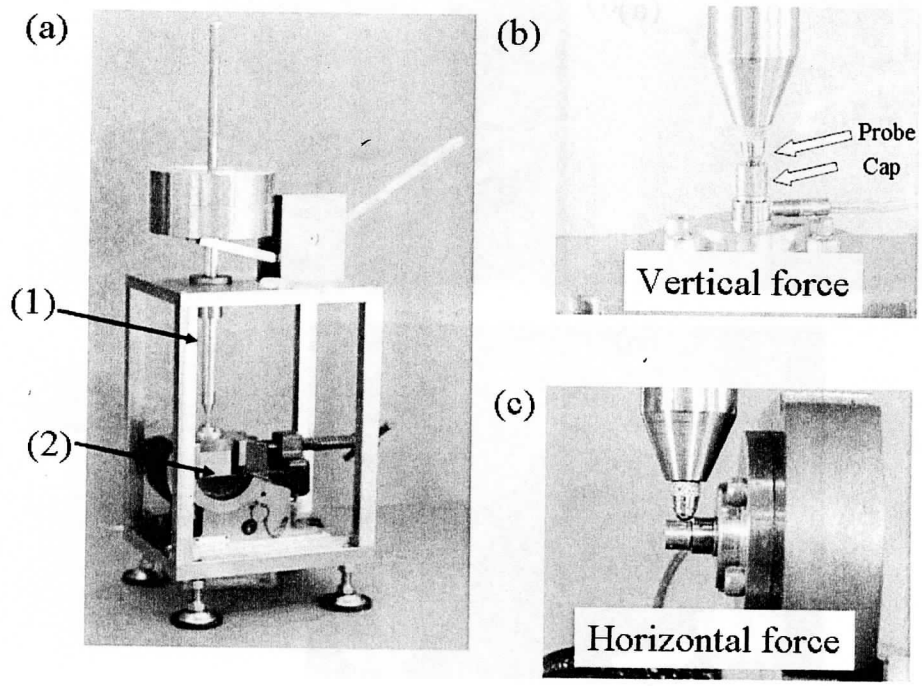

Fig. 2 (a) Proofreading apparatus: (1) ball spline with probe and (2) vise with variable angle (–15 to 130°). (b) Close-up during loading for vertical measurement; load point becomes point contact. (c) Close-up during loading for horizontal measurement.

Fig. 3

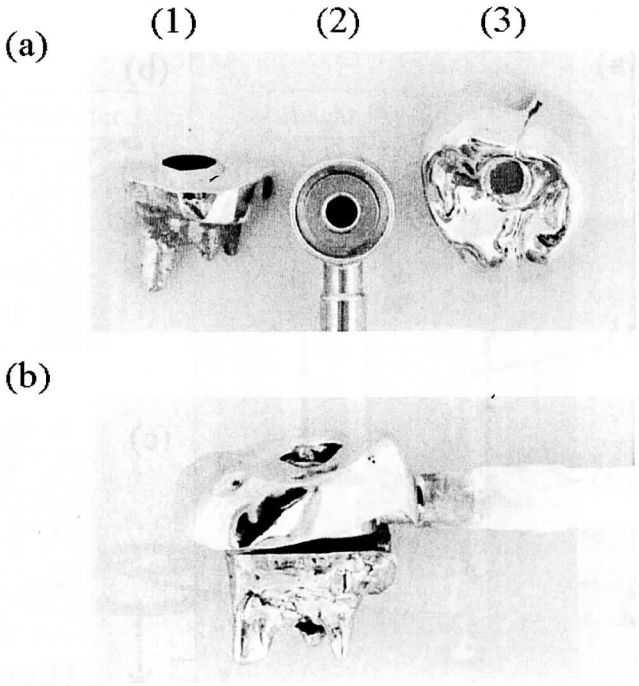

Fig. 3 Device for 3-D force measurement.

(a) Inner part (1) was similar to metal core, and force transducer (2) and outer part (3) were similar to metal tooth crown. (b) Photograph of measuring device in use. Outer part, force transducer, and inner part were joined with a steel screw.

Fig. 4

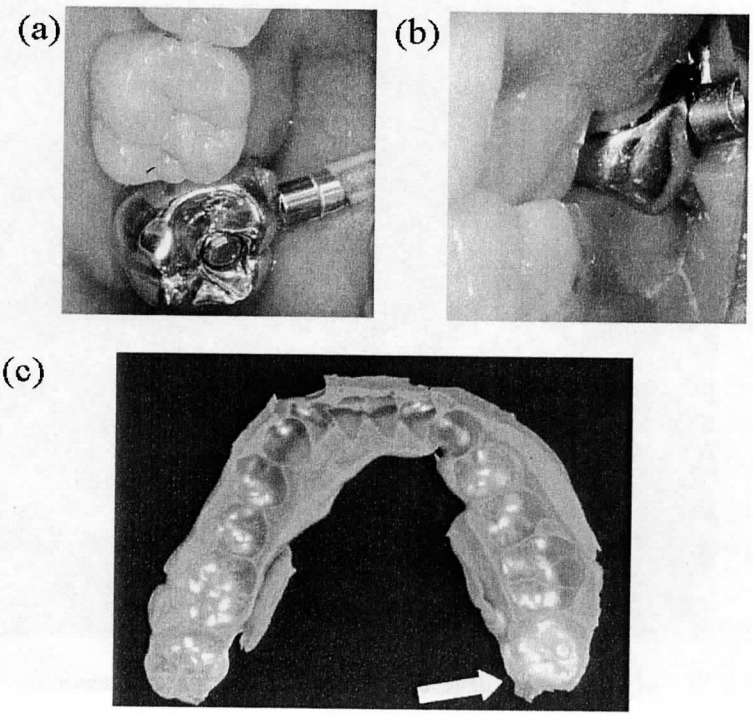

Fig. 4 Placement of transducer on tooth

(a) view from occlusal plane, (b) view from left side with mouth closed, and (c) view of occlusal contact (made of silicon rubber) with mouth closed as viewed from mandibular side with transmitted light. Measured tooth (white arrow) was equal to all other premolars and molars in terms of area of contact with opposing tooth.

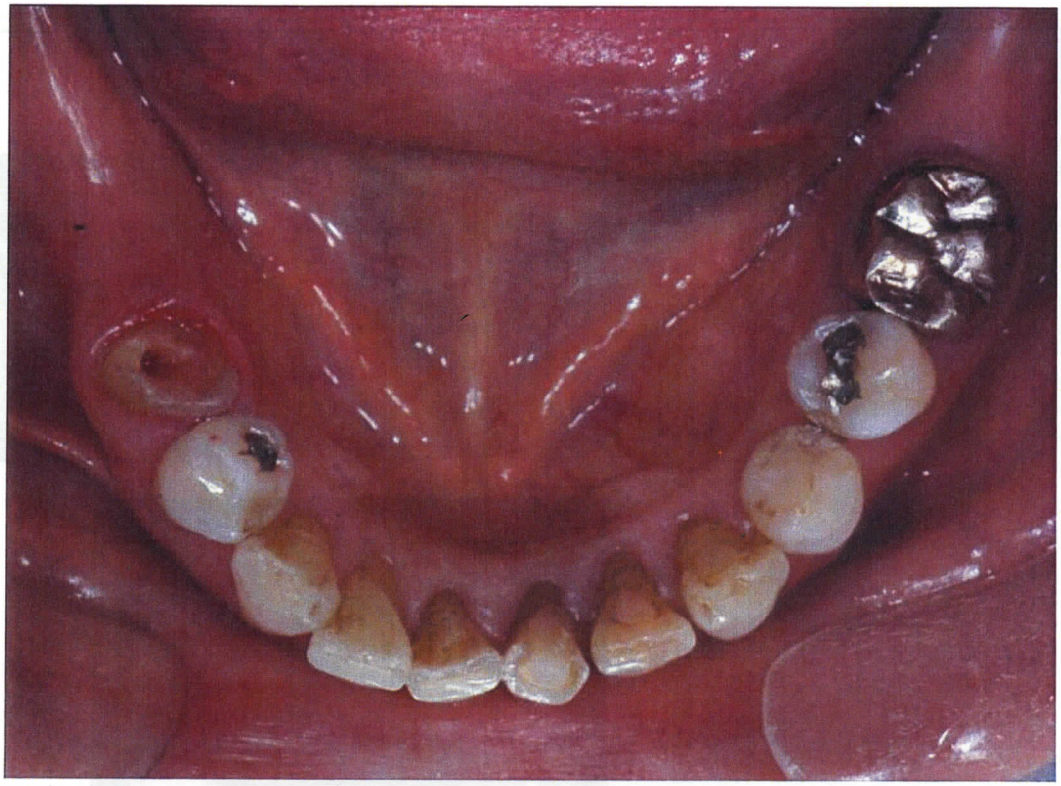

Fig. 5 Status of the mandible before setting the force measuring device in the RPD wearer

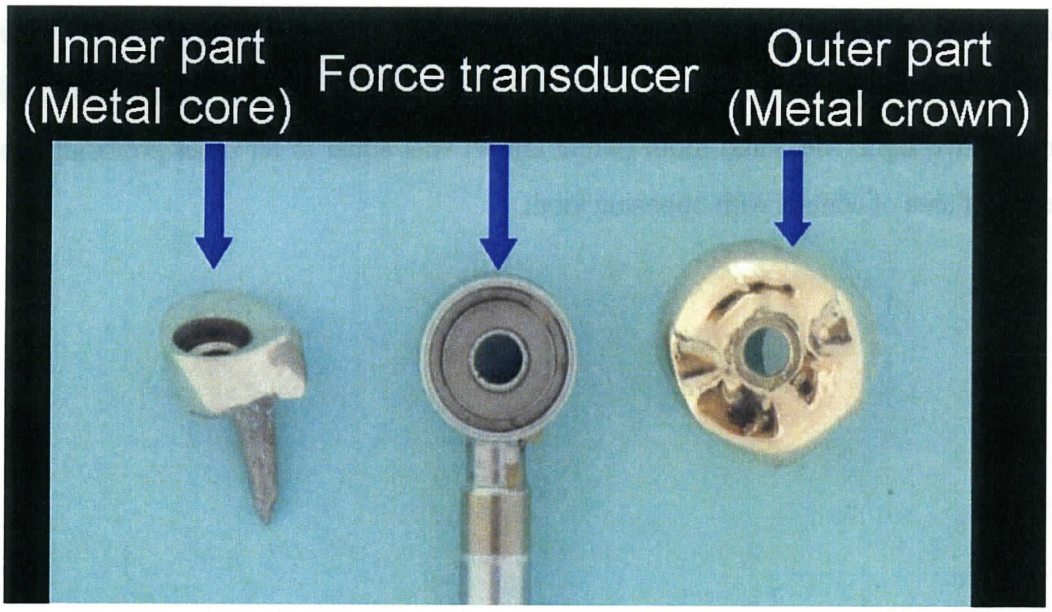

Fig. 6 Device for 3-D force measurement of the abutment tooth

Three parts were combined by a steel screw and fixed to the abutment tooth with temporary cement.

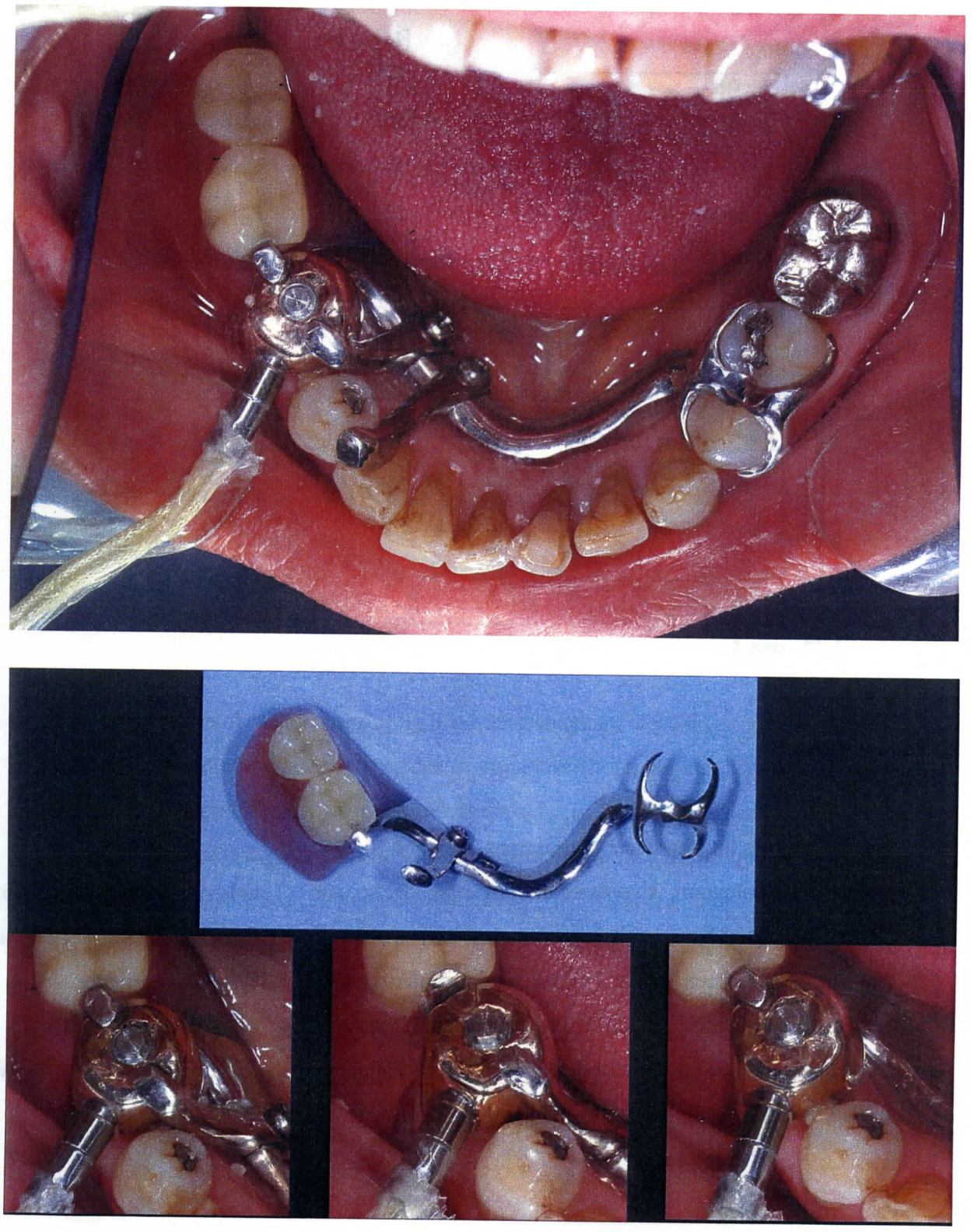

Fig. 7 Experimental partial denture with removable medial and distal rests

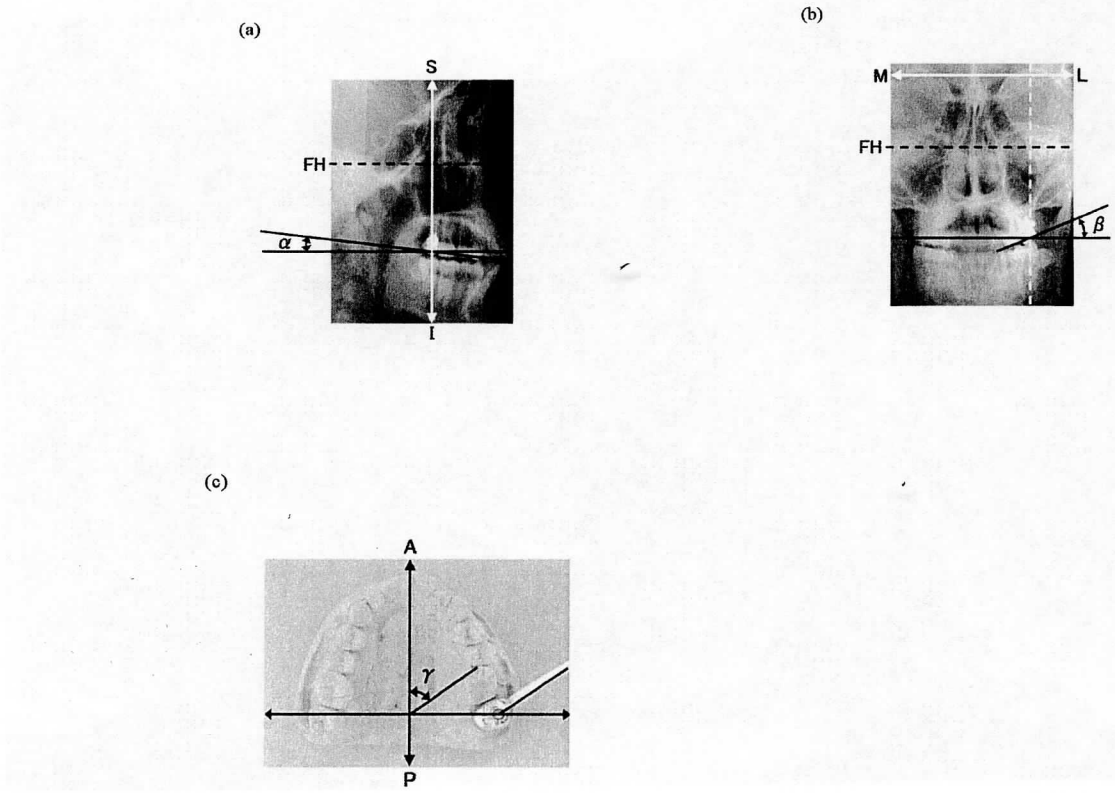

Fig. 8 Materials for transducer output transformation

(a) lateral cephalogram, (b) posteroanterior cephalogram, and (c) study cast. Rotation angles α and β were estimated from cephalograms; that of γ was estimated from study cast, on which the transducer had been affixed. The superior-inferior axis (S-I) was determined by a line perpendicular to the Frankfort-horizontal (FH) plane. The mediolateral axis (M-L) and anteroposterior axis (A-P) were determined by the FH plane. (Black dashed line: FH plane. White dashed line: line perpendicular to FH plane.)

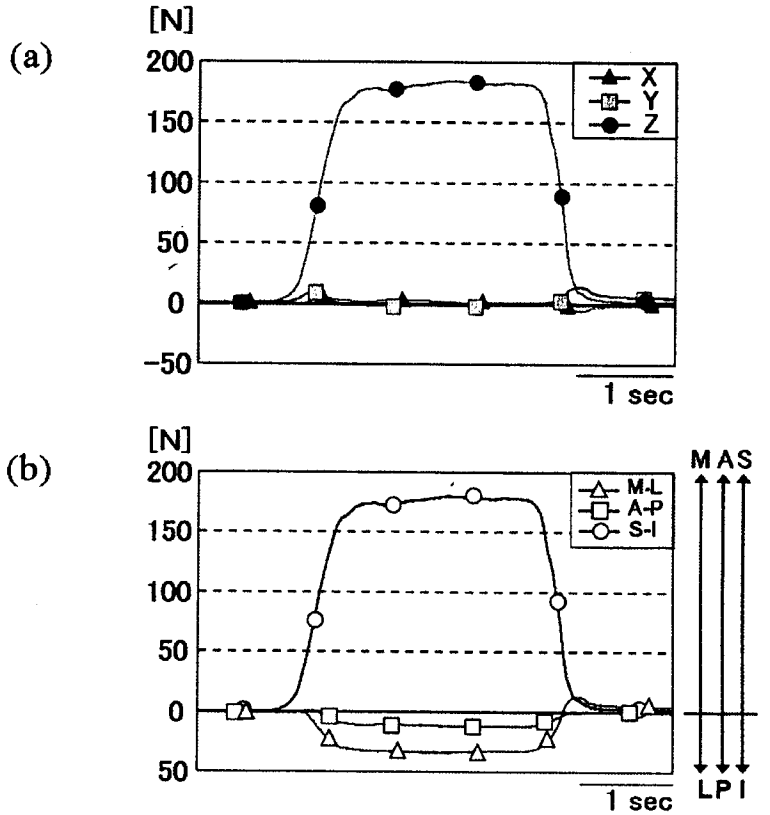

Fig. 9 Transformation of output data during maximum voluntary clenching

(a) example of raw output data; (b) example of transformed output data. Transducer output was transformed three-dimensionally using the rotation angles (α, β, and γ). After transformation, the data indicated the superior, posterior, and lateral directions.

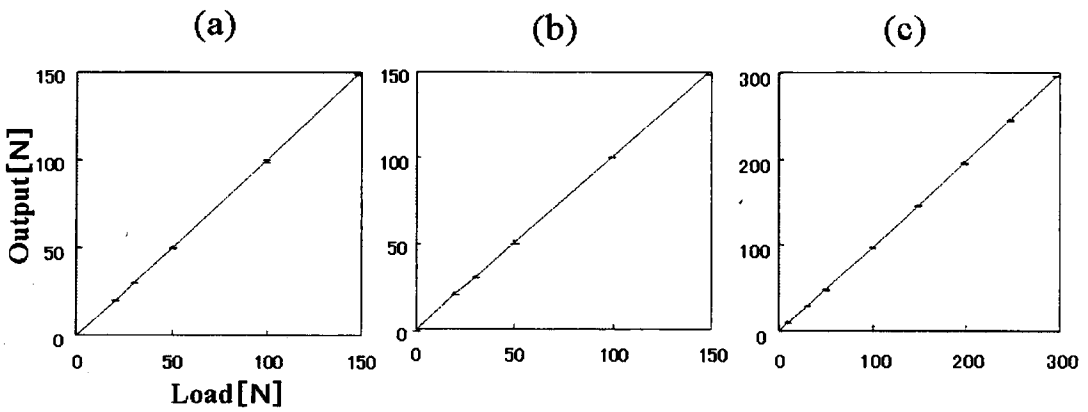

Fig. 10 Relationship between transducer output and actual load.

Correlation coefficients for (a) x-axis, (b) y-axis, and (c) z-axis were 0.99999, 0.99999, and 0.99996. Ten trials were carried out for each measurement condition.

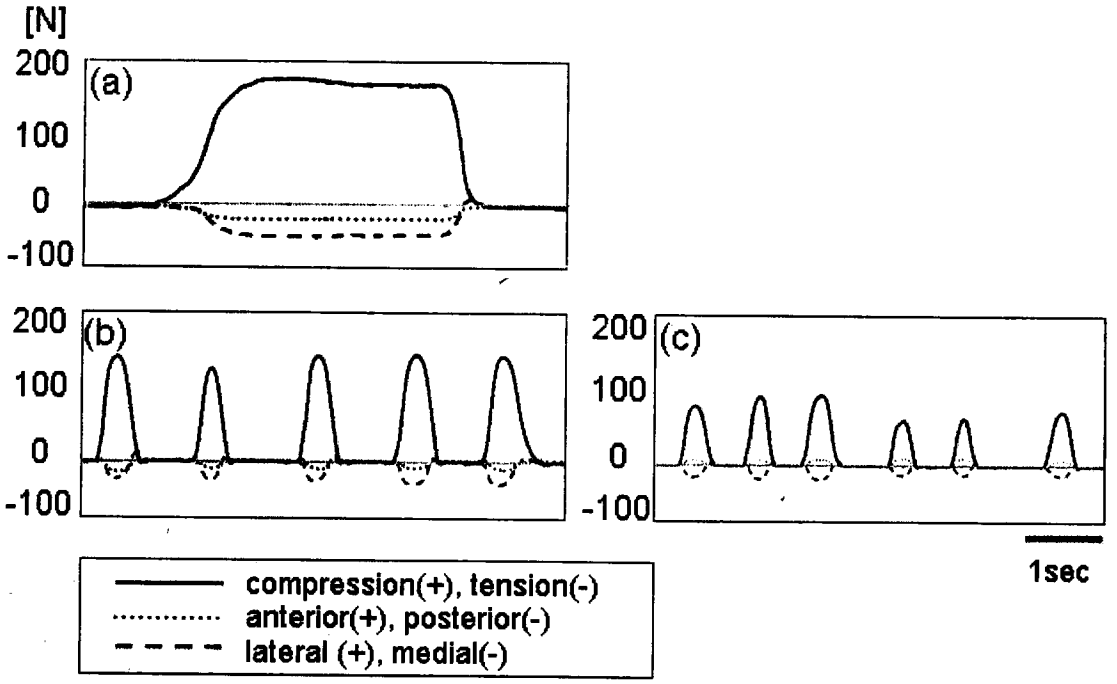

Fig.11 Example of calculated 3-D forces data for (a) MVC; (b) chewing caramel; (c) chewing peanut. MVC showed compressive, medial, and posterior directed forces with an apparent mediolateral overshoot. Caramel chewing showed mostly compressive force with tensile force at the end and medial and posterior directed forces with an apparent mediolateral overshoot at the end. Peanut chewing showed compressive, anterior, and medial forces. The plus signs indicate compression and anterior and lateral directed forces, and the minus signs indicate tension and posterior and medial directed forces.

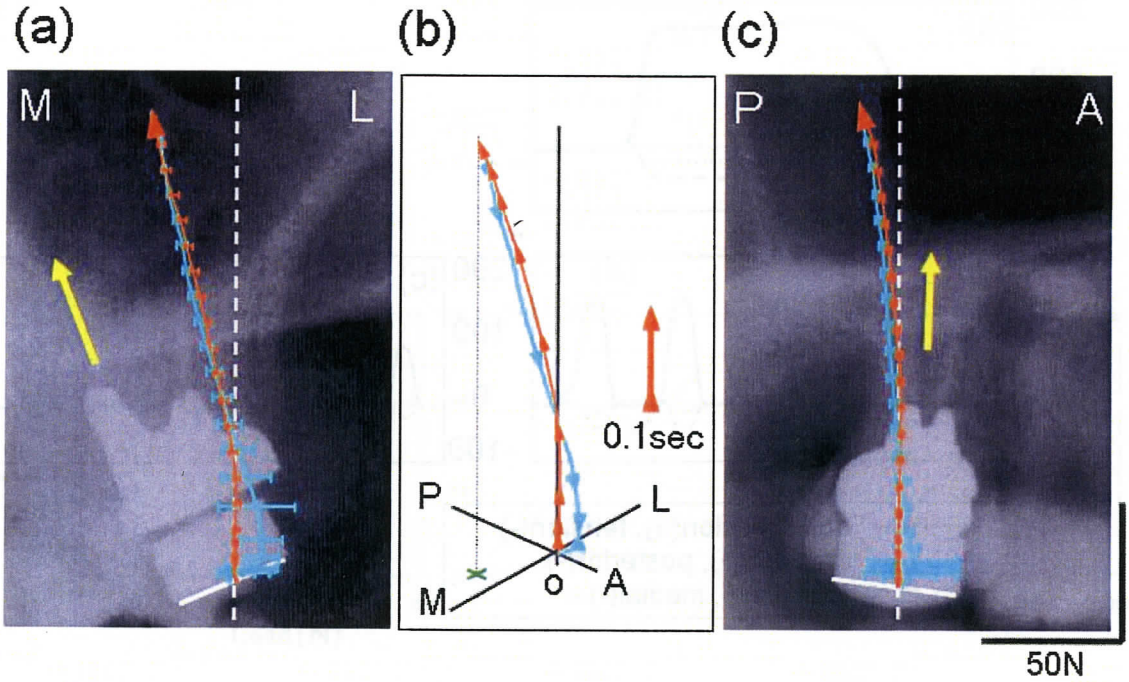

Fig.12 Vector locus during MVC

(a) coronal plane view; (b) 3-D view from medial-anterior position; (c) sagittal plane view. 3D force was converted into two 2-dimensional forces (coronal and sagittal plane). Top surface of each graph indicates F-H plane. White dashed line indicates direction perpendicular to F-H plane. Yellow arrow indicates palatal root of tooth. Orange locus and blue locus indicate closing and opening phases of vector, respeanut chewingtively. M: medial direction. L: lateral direction. P: posterior direction. A: anterior direction. O: vector origin (center of pressure receiver)

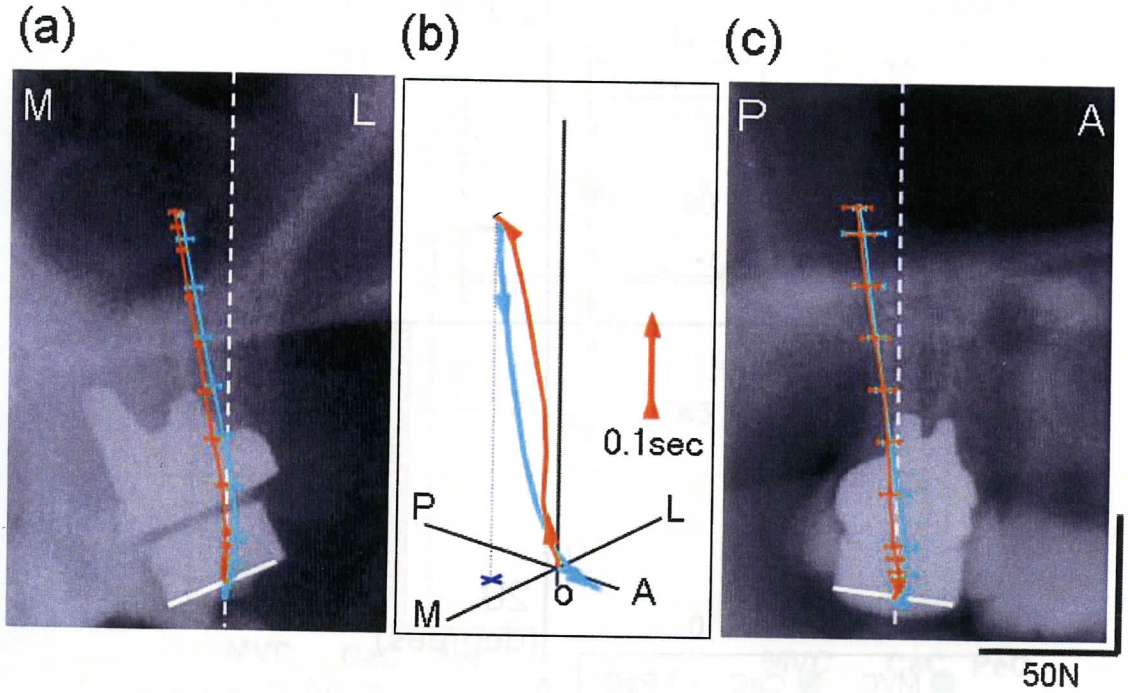

Fig.13 Vector locus for caramel chewing

(a) coronal plane view; (b) 3-D view from medial-anterior position; (c) sagittal plane view. Data expression and abbreviations are the same as in Fig. 12.

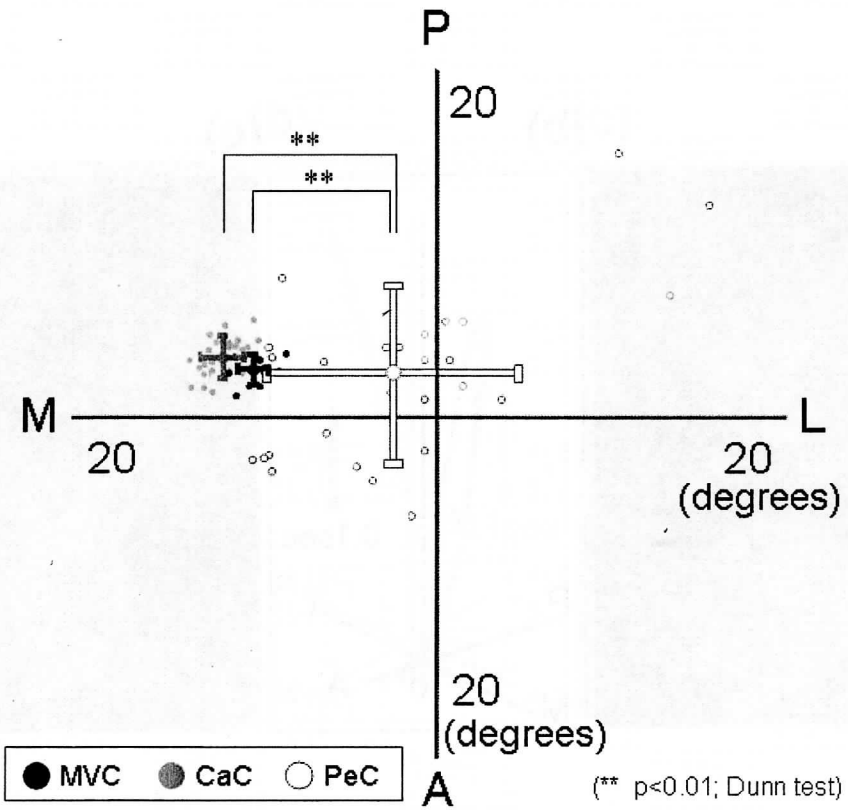

Fig.14 Mean vector directions for compressive force at maximum magnitude on the F-H plane. The number of sample data points for MVC, Caramel chewing, and Peanut chewing were 7, 35, and 10, respeanut chewingtively. Abbreviations are the same as in Fig. 12.

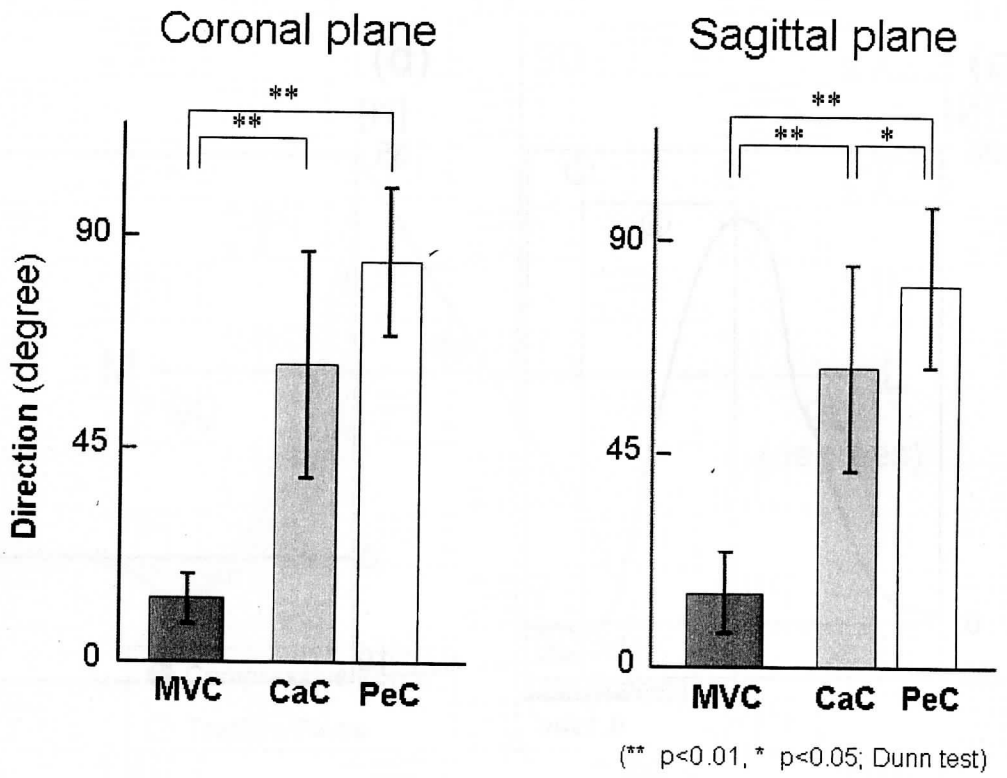

Fig. 15 Range of vector directions for compressive force during force-increasing phase.

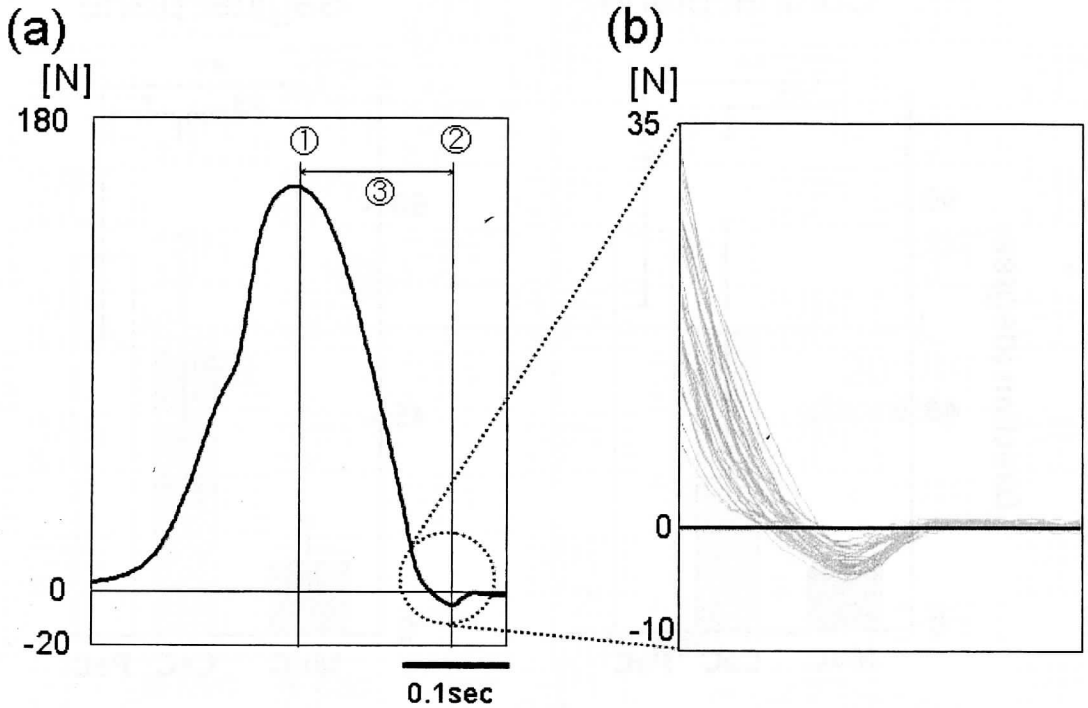

Fig. 16 (a) Example tensile and compressive forces measured during caramel chewing (compressive-tensile direction); (b) close-up of circled area in (a). ①: average maximum magnitude of compressive force, ②: maximum magnitude of tensile force, ③: 0.161±0.034 msec between ① and ②.

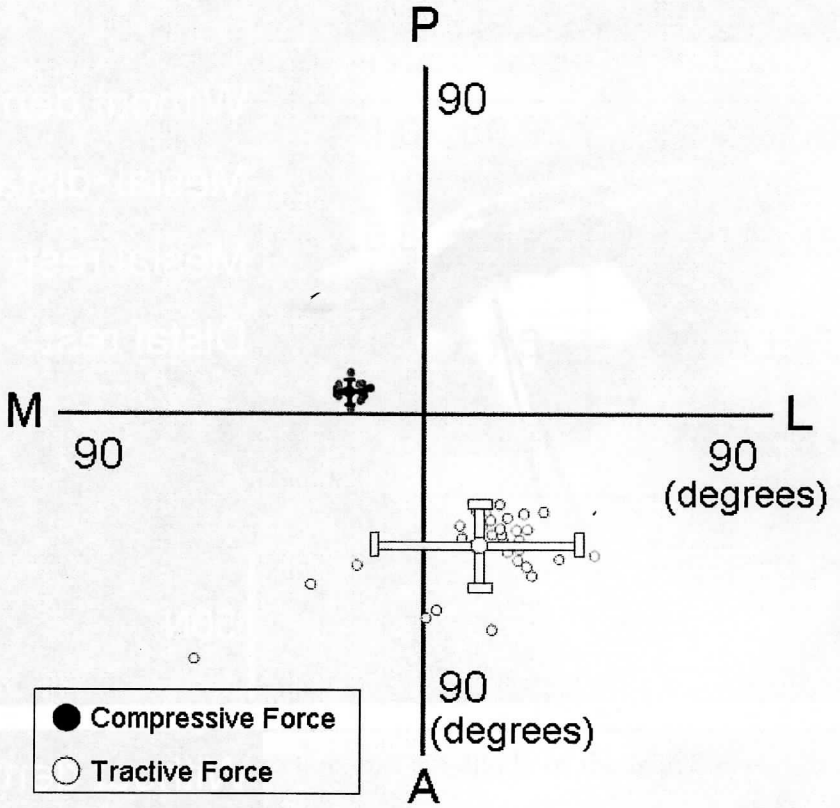

Fig.17 Vector directions at maximum magnitude during caramel chewing.

Abbreviations are the same as in Fig. 12.

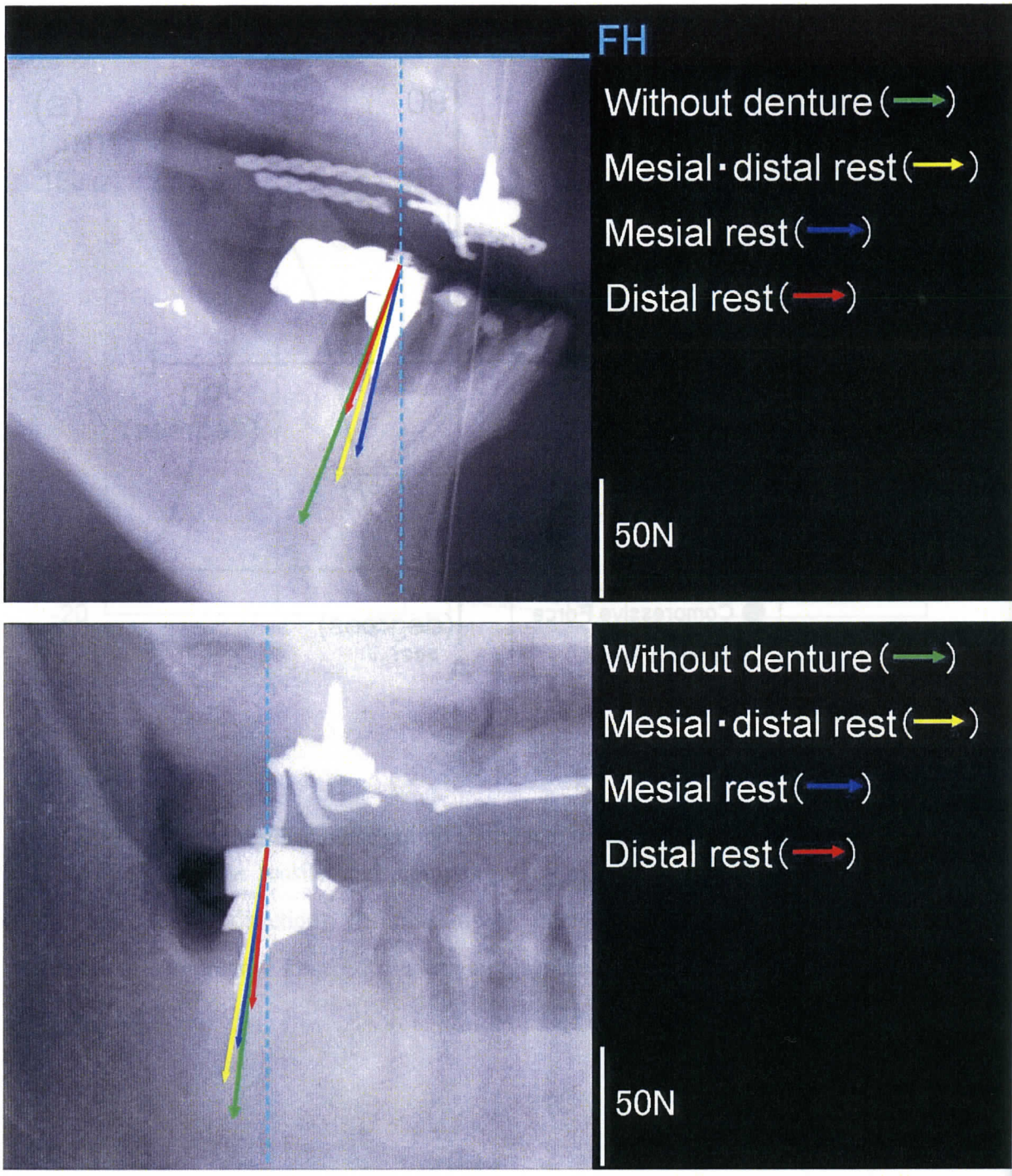

Fig.18 Force vector of the transmitted loads onto the abutment tooth.

(a)Force vectors on the sagittal plane, projected on the lateral cephalogram (b) Force vectors projected on the P-A cephalogram.

	Medio-lateral angle		Load(N)	
Without denture	21.0 ±0.9	**	112.9±8.1	*
Mesial·distal rest	16.8 ±0.9		93.5±15.3	
Mesial rest	12.8 ±1.6	**	87.6±13.8	
Distal rest	19.5 ±0.3		76.3±3.9	

(*; $p<0.05$, **; $p<0.01$, Dunn test)

(n=4)

Table 1 the mean values of the direction and amplitude of the loads measired at four different conditions in the sagittal plane.

	Medio-lateral angle	Load(N)	
Without denture	9.9 ±0.9	112.9±8.1	*
Mesial·distal rest	11.2 ±1.4	93.5±15.3	
Mesial rest	10.2 ±0.8	87.6±13.8	
Distal rest	9.0 ±1.0	76.3±3.9	

(*; $p<0.05$, Dunn test)

(n=4)

Table 2 the mean values of the direction and amplitude of the loads measired at four different conditions in the frontal plane.

6. 謝辞

本研究の遂行にあたり，ご協力を頂いた被験者各位ならびに東北大学大学院歯学研究科口腔システム補綴学分野教室員に，心から感謝し御礼を申し上げます．

＜研究成果資料＞